18èmes Journées Internationales de Thermique (JITH 2017)
Monastir (Tunisie), 25 - 27 Octobre 2017

Experimental and numerical study of electrochemical performance of solid oxide fuel cell

Abir Yahya [1,*], Hacen Dhahri[1], Khalifa Slimi [2]
[1] Thermal and Energetic Systems Studies Laboratory, National Engineering School, Monastir University, Ibn Eljazzar Street, 5019, Monastir, Tunisia
[2] Higher Institute of Transport and Logistics, Sousse University, Riadh City, P.O.Box 247, 4023, Sousse, Tunisia.
yahyaabir486@yahoo.com

Abstract: This paper treats an experimental and modeling study to predict the electrochemical performance of a Ni/YSZ supported planar SOFC with the air electrode made by LSFC-GDC. A complete electrochemical model is developed and calibrated on experiments to validate the numerical data. The fitting parameters extracted from the calibration study are used to validate the current-voltage characteristic of an SOFC tested with both H_2/H_2O and H_2/N_2 mixtures. Moreover, the effects of hydrogen molar fraction, fuel flow rate and operating temperature on the cell performance are investigated.

Mots clés : Experimental study,SOFC,electrochemical performance

1. Introduction

The adverse impact of conventional energy production methods like nuclear and fossil fuel combustion on the environment has led to an increased exploitation of alternative but above all greener and more sustainable energy sources. Solid oxide fuel cells, with advantages of low pollutant emission and high efficiency, are identified as a promising technology for power generation.

The electrochemical characteristics are very important for the SOFC design, which directly affect the cell power generation performance. In some electrochemical models, the electrode exchange current density, one of the most important parameters in the mathematical description of the activation overpotential, is assumed to be independent of operating parameters (e.g., temperature, pressure and gas composition) and cell's microstructural properties of the electrodes such as porosity and pore size [1,2].

In some modeling works, the concentration overpotential is ignored as the gas diffusion in the electrode is believed to be an efficient process [3, 4]. In other works, the concentration overpotential is predicted using limiting current density, which is estimated as constant [5,6] or a function to gas concentration, pressure, effective diffusion coefficient, geometrical structures of SOFC electrodes and temperature [7,8]. Neglecting the concentration loss can be unreasonable, especially for SOFCs supported on thick electrode layers, because the reactant concentration and current density vary sharply along the flow channel of fuel cell.

Several electrochemical models combining Butler-Volmer equation, diffusion models (i.e., Fick's) and Ohm's law to obtain the activation, concentration and ohmic overpotentials have been developed in order to solve the above described limitation in the evaluation of SOFC overpotentials for electrode-supported cells [9-11]. This approach has been proven to be successful in the simulation of SOFCs electrochemical behavior, as a good agreement is usually obtained between simulated results and experimental data for this type of models.

In the present work we introduce a complete electrochemical model of a solid oxide fuel cell. The model was first calibrated and validated based on experimental data using a commercial-size, anode-supported SOFC. The fitting parameters extracted from the calibration study can precisely simulate the current–voltage characteristic of the SOFC tested with both H_2/H_2O and H_2/N_2 mixtures.

Then, sensitivity tests shows the effect of operating parameters, such as fuel flow rate and operating temperature, on the voltage-current density and performance characteristic.

2. Experimental setup

The performance of a commercial fuel electrode-supported solid oxide cell (SOLIDpower, Italy) was investigated with H2/H2O/N2 mixtures by measuring the current-voltage characteristic of the cell at different temperatures. Experiments were performed in Politecnico di Torino.

The cell is circular-shaped with a diameter of 80 mm and an active surface area of ~ 47 cm2. The anode consists of a Ni/8YSZ porous layer (240 μm thickness) that provides the support for the 8YSZ thin electrolyte (8 μm dense layer) and the cathode, which is a 50 μm porous layer made by LSCF-GDC.

Experiments were performed in a temperature-controlled oven. The cell was placed in an unsealed alumina test-fixture providing radial gas distribution from the cell center – where the gas inlet is located – to the border. Metallic grids of nickel (anode) and platinum (cathode) were used for current collection, while the electrodes' voltage was measured with two separate sensing wires contacting the cathodic and anodic grids. A thermocouple was located in the cell center near the anode surface, providing the temperature of the experiment. Further details on the test setup can be found in previous study by co-authors [12].

The design of the experimental session is presented in Table 1. The anode was fed with a mixture of H2/H2O/N2 with different flow rates and fixed humidity (4%), while the cathode was fed with a fixed flow of dry air (1500 NmL min-1) in all the characterizations.. The polarization curves were measured first at 800 °C following the order reported in Table 1, then temperature was decreased by 50 °C with a ramp of 30 °C/h and the procedure was repeated until 700 °C. The experiments were performed in galvanostatic mode and current-voltage characteristics were obtained by varying the cell current with steps of 1 A (hold for 60 s each) using an electronic load (PLZ 664, Kikusui, Japan) from 0% FU (fuel utilization) to 50% FU.

Table 1: Experimental session.

Anode flow rate (NmL min^{-1})	**H_2 [%]**	**H_2O [%]**	**N_2 [%]**
For H_2/H_2O mixture			
800	96	4	0
500	96	4	0
400	96	4	0
500	80	20	0
500	40	60	0
For $H_2/H_2O/N_2$ mixture			
500	67	4	29
500	58	4	38
500	48	4	48
500	37	4	59

3. The electrochemical model

The electrochemical model uses Bulter-Volmer equation, Fick's model and Ohm's law for the description of the activation, concentration and ohmic overpotentials, respectively. Taking into account all the overpotential effects in a solid oxide fuel cell, the cell potential is given by

$$\mathrm{V} = E - \eta_{act,a} - \eta_{act,c} - \eta_{con,a} - \eta_{con,c} \quad (1)$$

3.1. Equilibrium potential

The equilibrium voltage of a SOFC can be expressed by the Nernst equation

$$\mathrm{E} = E_0 + \frac{RT}{2F} \ln\left(\frac{P^0_{H_2}\left(P^0_{O_2}\right)^{\frac{1}{2}}}{P^0_{H_2O}}\right) \quad (2)$$

Where R is the universal gas constant and F is the Faraday constant. E_0 is the reversible potential of the cell, which depends on the standard-state free energy variation of the electrochemical reaction, and can be numerically expressed as a function of the temperature [13].

$$E_0 = 1.253 - 2.4516 \times 10^{-4} T \quad (3)$$

3.2. Activation overpotential

Activation polarization is controlled by the electrode kinetics at the reaction site, which are assumed to be localed at the electrode-electrolyte interface. This polarization is directly related to the activation or charge-transfer polarization, which is due to the transfer of charges between the electronic and the ionic conductors. Activation polarization is given by the Butler–Volmer equation [14]:

$$J = J_0 \left[exp\left(\frac{\alpha z F \eta_{act}}{RT}\right) - exp\left(-\frac{(1-\alpha) z F \eta_{act}}{RT}\right)\right] \tag{4}$$

The activation overpotentials of the anode and cathode can be written as

$$\eta_{act,i} = \frac{RT}{\alpha_i F} sinh^{-1}\left(\frac{J}{2J_{0,i}}\right) = \frac{RT}{\alpha_i F} ln\left[\frac{J}{2J_{0,i}} + \sqrt{\left(\frac{J}{2J_{0,i}}\right)^2 + 1}\right], \quad i = a, c \tag{5}$$

where $J_{0,i}$ is the exchange current density that represents the readiness of an electrode to proceed with electrochemical reaction and it can be expressed as [19]:

$$J_{0,a} = \gamma_a \times \left(\frac{P_{H_2}}{P_{ref}}\right)^a \times \left(\frac{P_{H_2O}}{P_{ref}}\right)^b exp\left(-\frac{E_{act,a}}{RT}\right) \tag{6}$$

$$J_{0,c} = \gamma_c \times \left(\frac{P_{O_2}}{P_{ref}}\right)^c exp\left(-\frac{E_{act,c}}{RT}\right) \tag{7}$$

where $E_{act,a}$ and $E_{act,c}$ are the activation energy levels at the anode and cathode [15], γ_a and γ_c are the coefficients for exchange current density for anode and cathode; and a, b and c are exponential coefficients for the concentration dependency.

3.3. Concentration overpotential

Concentration polarization occurs when the fuel is consumed at the electrode–electrolyte interface, and the gas concentration decreases at the reaction sites [1,2].

The concentration overpotentials can be expressed as a function of the gas partial pressure difference between the electrode surface and the electrode-electrolyte interface.

$$\eta_{con,a} = \frac{RT}{2F} ln\left(\frac{P^0_{H_2} P_{H_2O}}{P_{H_2} P^0_{H_2O}}\right) \tag{8}$$

$$\eta_{con,c} = \frac{RT}{4F} ln\left(\frac{P^0_{O_2}}{P_{O_2}}\right) \tag{9}$$

The partial pressure of water and hydrogen is calculated by :

$$P_{H_2} = P^0_{H_2} - \frac{RT d_a}{2F D_{H_2,e}} J \tag{10}$$

$$P_{H_2O} = P^0_{H_2O} + \frac{RT d_a}{2F D_{H_2O,e}} J \tag{11}$$

where J is the current density of the cell and $D_{i,e}$ is a global diffusion coefficient for the i species that takes inti account both molecular and Knudsen diffusivity.

The partial pressure of oxygen at the cathode reaction sites is calculated by solving the Fick's diffusion equation and imposing the oxygen concentration on the electrode's surface:

$$P_{O_2} = \frac{p_c}{\delta_{O_2}} - \left(\frac{p_c}{\delta_{O_2}} - P^0_{O_2}\right) exp\left(\frac{\delta_{O_2} RT d_c J}{4F D_{c,e} p_c}\right) \tag{12}$$

3.4. Ohmic overpotential

Ohmic losses occur because of the resistance to the flow of ions in the electrolyte and the resistance to flow of electrons through the electrode materials. Ohmic polarization obeys Ohm's law and is given by [16]:

$$\eta_{ohmic} = R_{ohm} J = \left(\frac{d_a}{\sigma_a} + \frac{d_c}{\sigma_c} + \frac{d_e}{\sigma_e}\right) J \tag{13}$$

where d_a, $d_c$and d_e are the thickness of anode, cathode and electrolyte, respectively; σ_a, σ_c and $\sigma_e$are the electrical and ionic conductivities of the SOFC components [17] .

$$\sigma_a = \frac{9.5\ 10^7}{T} exp\left(-\frac{1150}{T}\right) \quad (14)$$

$$\sigma_c = \frac{4.2\ 10^7}{T} exp\left(-\frac{1200}{T}\right) \quad (15)$$

$$\sigma_e = 3.34\ 10^4 exp\left(-\frac{10300}{T}\right) \quad (16)$$

4. Results and discussion

4.1. Calibration and validation

In this section, we describe the fitting process employed to identify the values of the electrochemical parameters used for the simulation. The best-fitting serves to minimize the root-mean-square error between experimental and simulated J–V characteristics.

In the literature, the concentration parameters a and b vary significantly while c is generally set equal to 0.25; while Mogensen's model chooses a=b=1 [9,18]. While recently experimental works report lower values a=0.11 and b=0.67 [15] and Yamamura's model specifies a=1 and b=-0.5 [19,20].

Yamamura's values are used firstly in the present work to simulate fuel cell polarizations at 750 °C with fuel flow rate of 500 N ml/min for different fuel compositions (i.e., H2/H2O ratios).

The values of γ_a and γ_c are guessed in goal to obtain satisfactory agreement between experimental and numerical J–V curves. The electrochemical parameters for the different studied cases are reported in Table 2.

Figure 1a shows the experimental data and two iterations of the fitting process; case 1 and 2. As illustrated by this figure, both case 1 and 2 over predict the mean current density of SOFC with 80% H2 and 40% H2.

In case 3, the value of γ_c is changed. It is found that case 3 worsens the agreement of both 80% H2 and 40% H2 SOFC (see fig 1b).

In order to get a better fitting, the values of γ_a and γ_c are changed simultaneously is assumed in case 4. As indicated in Figure 1c, the results of case 4 improve compared to those of case 1, reducing the performance overestimation of the latter.

After several iterations represented by case 1, case 2, case 3 and case 4, we conclude that there is no pair values of γ_a and γ_c that makes a good agreement between numerical and experimental data. This conclusion underlines to Yamamura's values as the cause of this underperformance.

In case 5, we replace Yamamura's values of a,b and c by those in the work of Utz et al [15]. As shown in Figure 1d, the results of case 5 are better than those of case 4.

Mogensen's model is used (a=b=1, c=0.25) in a fitting process to provide a good fit of the experimental data both for low and high steam concentrations in SOFC. The best fit is that shown in Figure 2 for the electrochemical values reported in Table 3. Figure 2 shows good agreement between simulated and experimental results with a mean error of 2%.

As the dependence of concentration overpotential on molar fraction is more pronounced than that of the activation overpotential, a smaller voltage loss and higher power density could be obtained at high molar fraction, as shown by the modeling and experimental results presented in Fig 2.

Table 2.Electrochemical parameters for different cases.

Parameter	Case 1	Case 2	Case 3	Case 4	Case 5
$E_{act,a}$	100	100	100	100	100
α_a	0.4	0.4	0.4	0.4	0.4
γ_a	$5\ 10^9$	$1.5\ 10^{10}$	$5\ 10^9$	$1.5\ 10^{10}$	$1.5\ 10^{10}$
a	1	1	1	1	0.11
b	-0.5	-0.5	-0.5	-0.5	0.67
c	0.25	0.25	0.25	0.25	0.25
$E_{act,c}$	120	120	120	120	120
α_c	1	1	1	1	1
γ_c	$4\ 10^9$	$4\ 10^9$	$1.5\ 10^{10}$	$2\ 10^9$	$2\ 10^9$

Table 3. Best fitting parameters for H2/H2O mixtures.

Parameter	
$E_{act,a}$	100
α_a	0.4
γ_a	$5\ 10^9$
a	1
b	1
c	0.25
$E_{act,c}$	120
α_c	1
γ_c	$2\ 10^9$

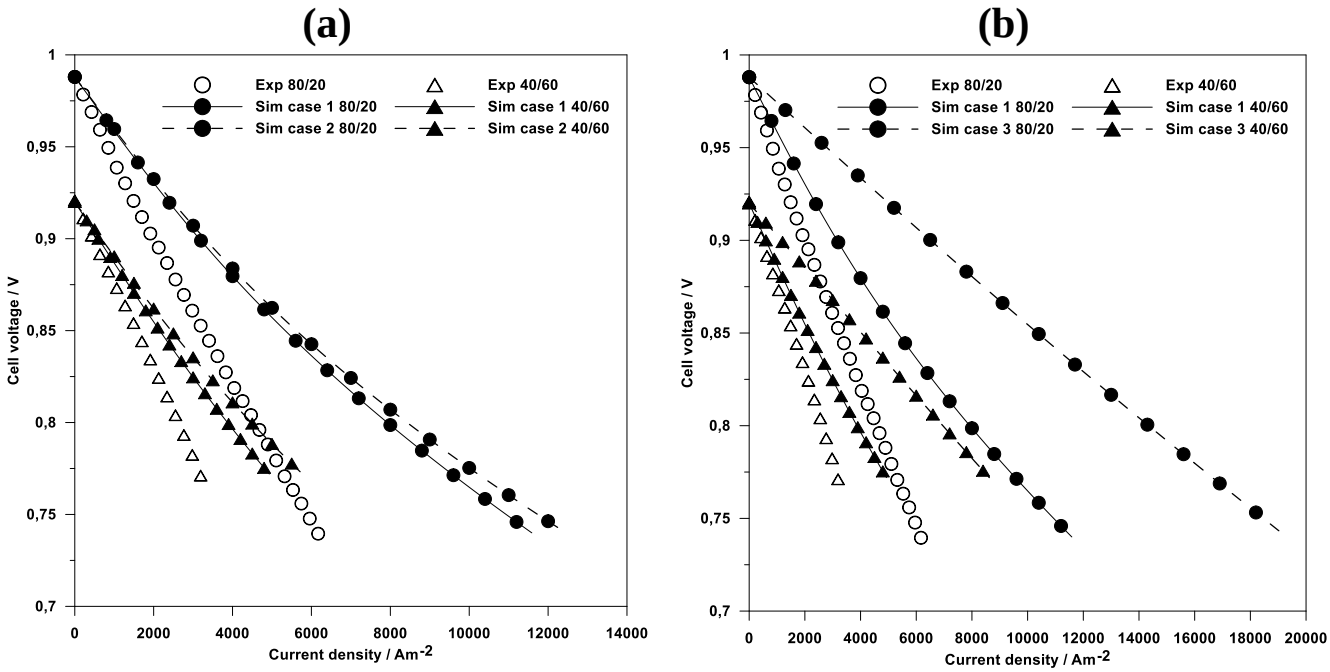

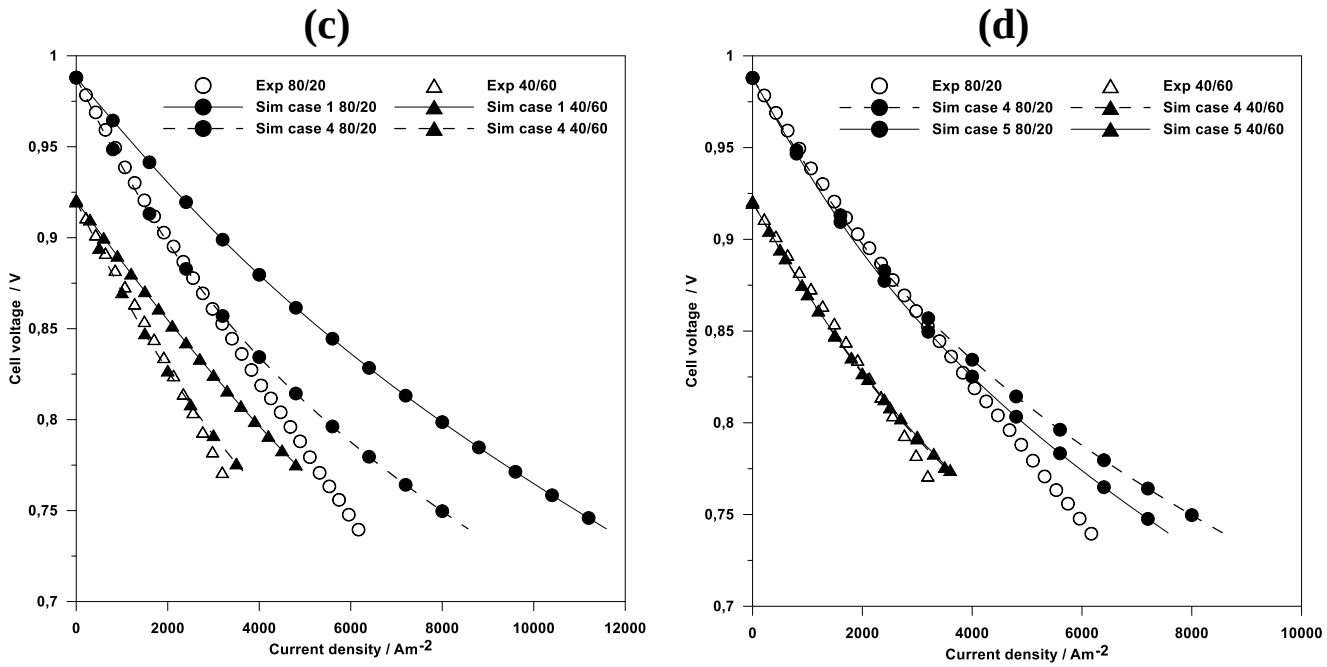

Fig. 1. J-V curves for 4 cases of fitting with H_2/H_2O mixtures.

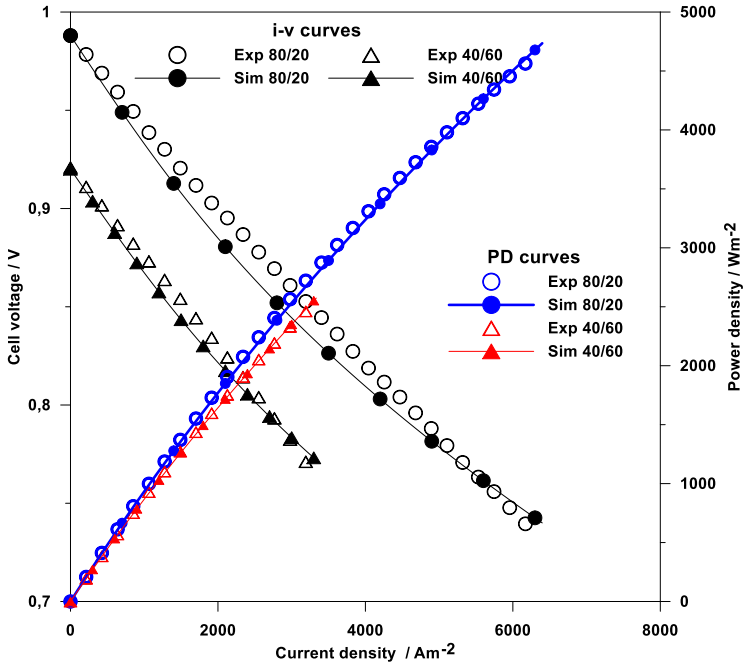

Fig.2. Experimental and simulated polarization and power density curves for SOFC with H_2/H_2O mixtures.

For the mixture H_2/N_2, a model calibration has been performed through the identification of the concentration dependency values a, b and c and the values of γ_a and γ_c. The best fit is that shown in fig 3 for the best fitting parameters reported in table 4.

Experiments are investigated at temperature of 750 °C. The fuel electrode was fed with 500 N ml/min of gas composed by mixtures H_2/N_2. The air electrode is fed with 1500 N ml/min of dry air. It is clear from Fig 4 that

the dilution with nitrogen does not influence strongly the fuel cell operation at low and medium current densities, whereas it produces higher impact at high current density**.**

Table 4. Best fitting parameters for H2/N2 mixtures.

Parameter	
$E_{act,a}$	100
α_a	0.4
γ_a	1.2 10^{10}
a	1
b	1
c	0.25
$E_{act,c}$	120
α_c	1
γ_c	20 10^{10}

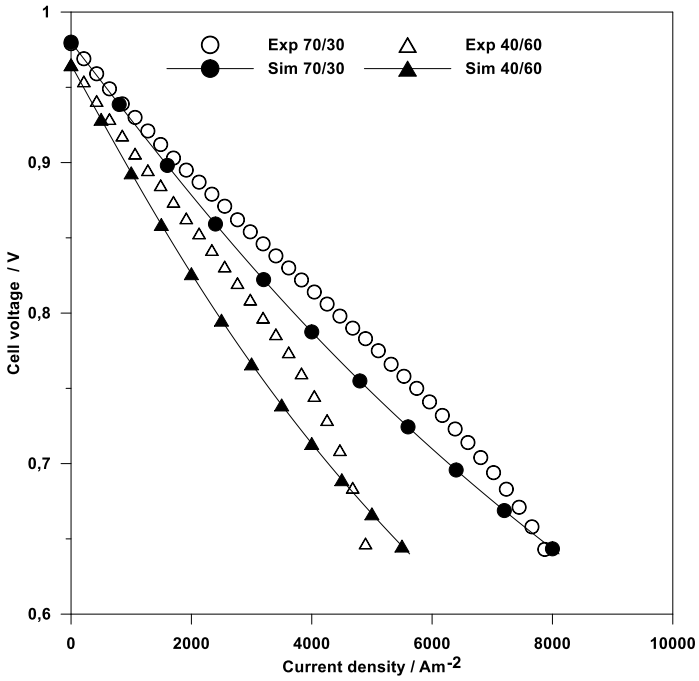

Fig. 3. Experimental and simulated polarization curves for SOFC with H_2/N_2 mixtures.

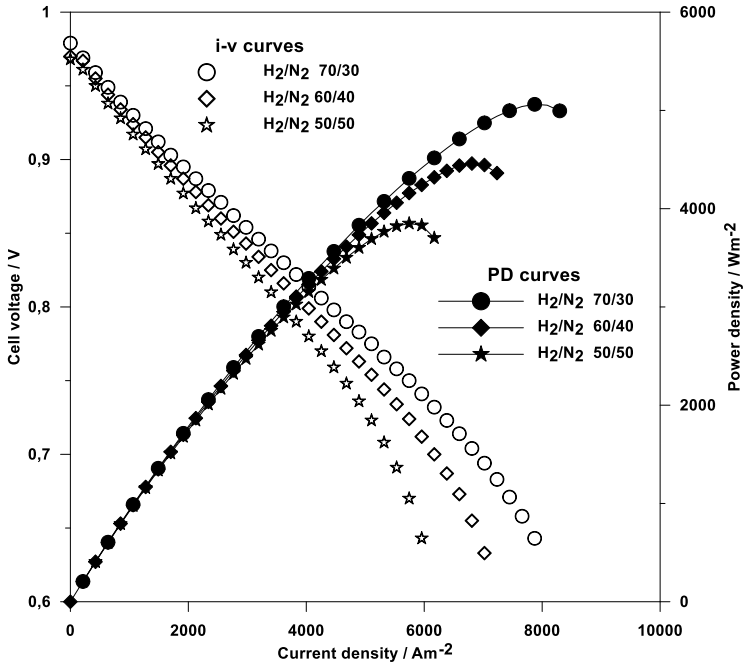

Fig. 4. Effect of hydrogen molar fraction on cell voltage and power density.

4.2. Flow rate effect

Fig 5 shows the polarization curves for the SOFC fed by mixture 96% H_2, 4% H_2O at different fuel flow rate. As shown, polarization losses increase as the fuel flow rate decreases. We note also that changing the fuel flow rate has effect on the activation and concentration polarizations, since they are strong functions of the gas mixture composition and concentration. So the operation at high flow rate is required to achieve high efficiencies.

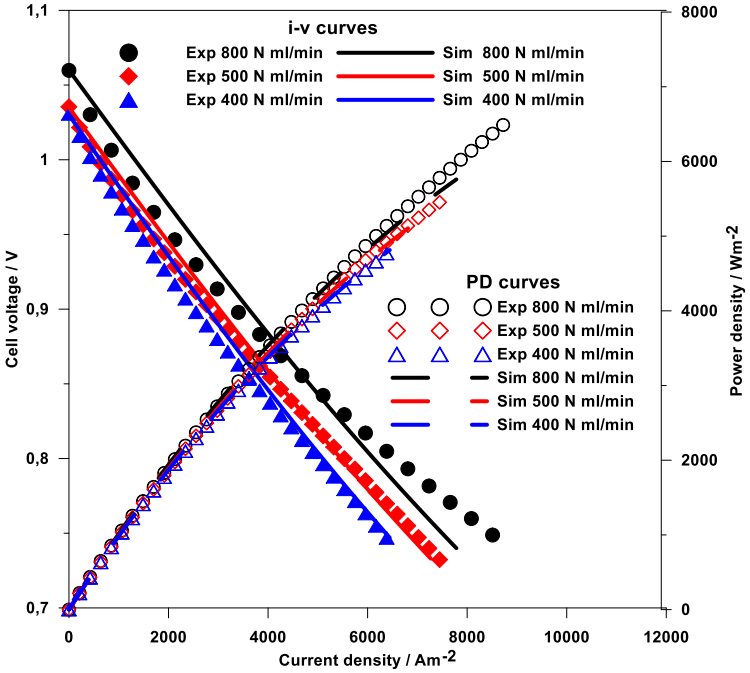

Fig. 5.Effect of fuel flow rate on cell voltage and power density.

4.3. Operating temperature effect

The performance of SOFC depends strongly on the operating temperature as demonstrated in Figure 6 because the three polarization losses are affected by the temperature. Decreasing the inlet temperature significantly promotes the cell ohmic losses because the ionic conductivity of the electrolyte is very sensitive to the temperature. Moreover, the activation overpotential is found to increase when the operating temperature reduce due to lower activity of the cell catalyst and surface reactions. It is also clear from Fig 6 that a higher power density can be obtained at a higher temperature.

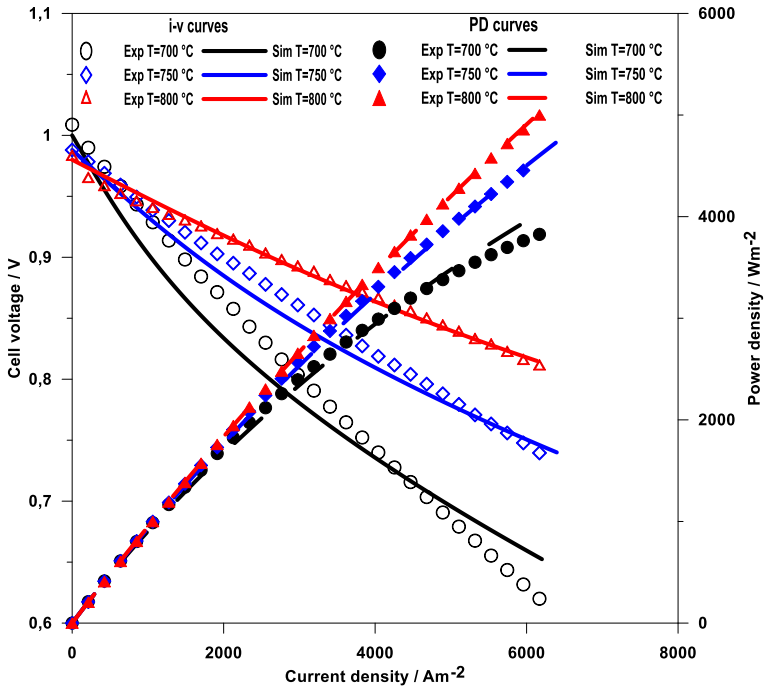

Fig. 6. Effect of operating temperature on cell voltage and power density.

5. Conclusion

In this work, we have presented a numerical and experimental study of solid oxide fuel cell performance. The validation of a numerical model involves the fitting of electrochemical parameters which are then used to simulate current-voltage characteristics of SOFC with H_2/H_2O and H_2/N_2 mixtures and a good agreement is found between numerical and experimental results. The impacts of operating parameters on cell voltage and power density are discussed; when the hydrogen molar fraction rises, the power density represents an increasing tendency. Similarly, the cell performance improves with increasing of both fuel flow rate and operating temperature.

Nomenclature

a	Exponential coefficients	R_{ohm}	Electric resistivity, Ωm^2
b	Exponential coefficients	r	Mean pore radius , $\mu)$
c	Exponential coefficients	T	Temperarure, K
d_a	Thickness of anode , μm	V	Cell potentiel ,V

d_c	Thickness of cathode , μm	$\eta_{act,a}$	Activation overpotential of the anode, V
d_e	Thickness of electrolyte , μm	$\eta_{act,c}$	Activation overpotential of the cathode, V
$D_{i,e}$	Effective diffusion coefficient, m^2s^{-1}	$\eta_{con,a}$	Concentration overpotential of the anode, V
E	Equilibrium voltage , V	α_i	Transfer coefficient
E_0	Reversible potential, V	γ_a	Coefficients for exchange current density for anode
$E_{act,a}$	Activation energy at the anode ,J mol^{-1}	γ_c	Coefficients for exchange current density for cathode
$E_{act,c}$	Activation energy at the cathode,$Jmol^{-1}$	σ_a	Electrical conductivity, $\Omega^{-1}\ m^-$
F	Faraday constant	σ_c	Electrical conductivity , $\Omega^{-1}\ m^-$
J	Curent density (Am^{-2})	σ_e	Ionic conductivity , $\Omega^{-1}\ m^-$
$J_{0,i}$	Exchange current density, Am^{-2}	η_{ohmic}	Ohmic overpotential ,V
P	Pressure , bar	$\eta_{con,c}$	Concentration overpotential of the cathode ,V

References

[1] Hernandez-Racheco E, Singh D, Hutton PN, Patel N, Mann MD. A macro-level model for determining the performance characteristics of solid oxide fuel cells. J Power Sources 2004;138(1–2):174–86.

[2] Chan SH, Xia ZT. Polarization effects in electrolyte/electrode supported solid oxide fuel cells. J Appl Electrochem 2002;32(3): 339–47.

[3] Hofmann P, Panopoulos KD, Fryda LE, Kakaras E. Comparison between two methane reforming models applied to a quasi-two-dimensional planar solid oxide fuel cell model. Energy 2009;34:2151e7

[4] Song TW, Sohn JL, Kim JH, Kim TS, Ro ST, Suzuki K. Performance analysis of a tubular solid oxide fuel cell/micro gas turbine hybrid power system based on a quasi-two dimensional model. J Power Sources 2005;142:30e42.

[5] Bang-Møller C, Rokni M, Elmegaard B, Ahrenfeldt J, Henriksen UB. Decentralized combined heat and power production by two-stage biomass gasification and solid oxide fuel cells. Energy 2013;58:527-37

[6]Chakraborty UK. Static and dynamic modeling of solid oxide fuel cell using genetic programming. Energy 2009;34:740-51.

[7] Rokni M. Thermodynamic analysis of SOFC (solid oxide fuel cell)eStirling hybrid plants using alternative fuels. Energy 2013;61:87e97.

[8] Liso V, Olesen AC, Nielsen MP, Kær SK. Performance comparison between partial oxidation and methane steam reforming processes for solid oxide fuel cell (SOFC) micro combined heat and power (CHP) system. Energy 2011; 36: 4216e26

[9] Meng N,Michael KHL,Dennis YCL.Parametric study of solid oxide fuel cell performance.Energy conversion and managment 2007;(48):1525-1535

[10] Goldin, Graham M., et al. Multidimensional flow, thermal and chemical behavior in solid-oxide fuel cell button cells. Journal of Power Sources 187.1 (2009); 123-135.

[11] Elizalde-Blancas, Francisco, et al. Numerical modeling of SOFCs operating on biogas from biodigesters. International Journal of Hydrogen Energy 38.1 (2013); 377-384.

[12] D. Ferrero, A.Lanzini, P. Leone,M. Santarelli. Reversible operation of solid oxide cells under electrolysis and fuel cell modes: Experimental study and model validation. Chemical Engineering Journal 274 (2015): 143-155.

[13] Fuel cell handbook, 7th ed., EG&G Technical Services Inc., U.S. Department of Energy, Morgantown, (WV, USA), November 2004. pp. 57–60.

[14] C. Berger, Handbook of Fuel Cell Technology, Prentice-Hall, Englewood Cliffs, NJ, 1968

[15] Utz A, Stormer H, Leonide A, Weber A, Ivers-Tiffee E. Degradation and relaxation effectsofnipatternedanodesinH2–H2O atmosphere .J Electro chem Soc 2010;157(6):B920–30.

[16] Ferguson JR, Fiard JM, Herbin R. Three-dimensional numerical simulation for various geometries of solid oxide fuel cells. J Power Sources 1996; 58(2):109–22.

[17]K. Tseronis, I. Bonis, I.K. Kookos, C. Theodoropoulos. Parametric and transient analysis of non-isothermal, planar solid oxide fuel cells. International Journal of Hydrogen Energy 37 (2012); 530-547.

[18] Costamagna P, Honegger K. Modeling of solid oxide heat exchanger integrated stacks and simulation at high fuel utilization. J Electrochem Soc1998; 145(11): 3995–4007

[19] Andreassi L, Rubeo G, Ubertini S, Lunghi P, Bove R. Experimental and numerical analysis of a radial flow solid oxide fuel cell.IntJ Hydrogen Energy 2007;32(17):4559–74.

[20] Akhtar N, Decent S,Kendall K. Numerical modelling of methane-powered micro- tubular,single-chamber solid oxide fuel cell.JPowerSources2010;195(23): 7818–24.